[8] S. K. MAKSIMOV, T. I. LUKYANCHUK, and M. M. MYSHLYAEV, phys. stat. sol. (a) **24**, 409 (1974). S. K. MAKSIMOV and A. P. FILIPPOV, phys. stat. sol. (a) **61**, 175 (1980).
[9] A. K. HEAD, P. HUMBLE, L. M. CLARENBROUGH, A. J. MORTON, and C. T. FORWOOD, Computed Electron Micrographs and Defect Identification, North Holland Publ. Co, Amsterdam 1973.
[10] K. MARUKAWA, Phil. Mag. **A40**, 303 (1979).
[11] W. BOLLMANN, Phil. Mag. **13**, 935 (1966).
[12] J. P. HIRTH and J. LOTHE, Theory of Dislocations, McGraw-Hill Publ. Co., New York 1968.
[13] S. RUVIMOV and K. SCHEERSCHMIDT, Inst. Phys. Conf. Ser. (1993), to be published.
[14] D. HULL, Introduction of Dislocations, Pergamon Press, 1965 (p. 260).
[15] S. RUVIMOV and L. M. SOROKIN, Soviet Phys. – Solid State **26**, 278 (1984).
[16] G. H. ELSEN and M. ETTENBERG, in: Crystal Growth. Theory and Techniques, Vol. 2, Ed. C. H. L. GOODMANN, Plenum Press, New York 1978 (p. 8).
[17] B. S. YAVICH, I. N. KOCHNEV, P. P. BUINOV et al., Solid State Phenom. **19/20**, 587 (1991).
[18] M. WILKENS, in: Diffraction and Imaging Techniques in Materials Science, Ed. S. AMELINCKX, R. GEVERS, and J. VAN LANDUYT, North-Holland Publ. Co., Amsterdam 1978 (p. 185).

(Received November 29, 1993)

phys. stat. sol. (a) **141**, 269 (1994)

Subject classification: 61.14 and 61.70; S7.1

Max-Planck-Institut für Mikrostrukturphysik, Halle (Saale) [1])

Burgers Vector Determination in TEM by Using the Dislocation Parity Analysis

By

S. S. RUVIMOV [2]) and K. SCHEERSCHMIDT

A modified method of identifying the Burgers vector $\boldsymbol{b}$ is proposed, which is based on the extended analysis of dislocation contrast features. High voltage electron microscopy (HVEM) as well as the computer simulation of the electron micrographs are applied to study the contrast behaviour of mixed dislocations with a large screw component of the Burgers vector under different diffraction conditions in order to check the validity of the method proposed. The analysis of the contrast oscillations along inclined dislocations or the image shift relative to the projection of the dislocation line enables us to determine the 'dislocation parity' $P = \text{sgn}\,(\boldsymbol{l} \times \boldsymbol{b} \cdot \boldsymbol{B})$ while the halo contrast can be used to define the orientation of the 'additional half plane', which is characterized by the normal $\boldsymbol{e} = \boldsymbol{l} \times \boldsymbol{b}/|\boldsymbol{l} \times \boldsymbol{b}|$ to the glide plane. The parity and sgn $(\boldsymbol{g} \cdot \boldsymbol{e})$ analysis enables the unambiguous $\boldsymbol{b}$ vector determination whenever solely one invisibility criterion is applicable. The dislocation parameters in heterostructures are investigated by the above method.

Eine modifizierte Methode zur Bestimmung des Burgersvektors $\boldsymbol{b}$ wird vorgeschlagen, die auf einer detaillierten Analyse von Kontrasterscheinungen an Versetzungen beruht. Um die Gültigkeit der vorgeschlagenen Methode zu testen, wird sowohl die Hochspannungs-Elektronenmikroskopie (HVEM) als auch die Computersimulation der Abbildung zur Untersuchung des Kontrastverhaltens gemischter Versetzungen mit großem Schraubenanteil des Burgersvektors unter verschiedenen Beugungskontrastbedingungen verwendet. Die Analyse der Kontrastoszillationen entlang geneigter Versetzungen oder die Bildverschiebung relativ zur Projektion der Versetzungslinie ermöglichen die Bestimmung der „Versetzungsparität" $P = \text{sgn}\,(\boldsymbol{l} \times \boldsymbol{b} \cdot \boldsymbol{B})$, während der Halokontrast geeignet ist, die Orientierung einer „eingeschobenen Halbebene" zu definieren, d. h. die durch die Gleitebenennormale $\boldsymbol{e} = \boldsymbol{l} \times \boldsymbol{b}/|\boldsymbol{l} \times \boldsymbol{b}|$ gekennzeichnete Richtung. Wenn Kontrastauslöschung mindestens für einen Beugungsvektor erreicht werden kann, dann erlaubt die Analyse der Parität bzw. von sgn $(\boldsymbol{g} \cdot \boldsymbol{e})$ eine eindeutige Burgersvektorbestimmung. Mit der vorgeschlagenen Methode werden Versetzungsparameter in Heterostrukturen untersucht.

1. Introduction

In transmission electron microscopy (TEM) the Burgers vector of a dislocation is usually determined in at least three different ways. The first one is based on the invisibility criterion $\boldsymbol{g} \cdot \boldsymbol{b} = 0$, where $\boldsymbol{g}$ is the diffraction vector and $\boldsymbol{b}$ the Burgers vector [1, 2]. In general, two noncoplanar $\boldsymbol{g}$ vectors fulfilling the invisibility criterion are necessary and sufficient to unambiguously determine the $\boldsymbol{b}$-axis. Difficulties arise if the invisibility rules cannot be strictly applied to, e.g., anisotropic media, certain mixed or partial dislocations, many beam excitations, etc. [3]. The most important restriction, however, is the impossibility of generally determining the direction (or sense) of $\boldsymbol{b}$ by using the invisibility criterion. Thus it is necessary

[1]) Weinberg 2, D-06120 Halle (Saale), Federal Republic of Germany.
[2]) Permanent address: A. F. Ioffe Physico-Technical Institute, Russian Academy of Sciences, 194021 St. Petersburg, Russia.

to gain further information by analysing contrast details (e.g. image shift, contrast oscillations, symmetry) or by applying inside–outside [4 to 6] or halo contrast [7, 8] methods to define the direction of $\boldsymbol{b}$.

Image simulation or the matching technique [9] is the second way to determine the $\boldsymbol{b}$ vector. Being quite reliable without a parameter determination directly from the experiment or by using the other methods discussed here, this method has a degree of freedom far too high in the parameter space. The high degree of freedom can be reduced by the predominance of some of the parameters applying the invisibility rule or by analysing contrast details again.

The third way, proposed by Marukawa [10] makes use of characteristic image features such as the asymmetry related to the signs of $\boldsymbol{g} \cdot \boldsymbol{b}$ and $(\boldsymbol{g} \cdot \boldsymbol{b} \times \boldsymbol{l})$, where $\boldsymbol{l}$ is the dislocation line vector. Analysing the image asymmetry at different $\boldsymbol{g}$ reflections reveals that the probable orientation of the Burgers vector lies at a solid angle so small that it is possible to choose $\boldsymbol{b}$ directly from crystallographically allowable vectors. Though rather suitable to practical use the method has some restrictions, too. For example, it cannot be applied to dislocations lying parallel to the foil surface.

The direction of the Burgers vector $\boldsymbol{b}$ is always strictly associated with the line direction $\boldsymbol{l}$ in agreement with the FS/RH convention (finish–start/right hand) [11, 12], i.e. while the physical properties of the crystal containing a dislocation are known to be invariant to the change of the coordinate system, the sense of $\boldsymbol{b}$ and $\boldsymbol{l}$ as well as the related dislocation parameters change sign under coordinate inversion. Therefore, the practical determination of the dislocation sign may be unified by using another dislocation parameter directly characterizing the relevant physical properties (extrinsic–intrinsic, misfit, etc.).

The aim of the present paper is to modify the methods of the $\boldsymbol{b}$ determination in such a way that contrast analyses allow us to unambiguously define $\boldsymbol{b}$ whenever solely one invisibility criterion can be applied. Indeed, one $\boldsymbol{g}$ vector fulfilling the invisibility criterion can be found rather easily in most of the practical cases, implying also the projection of the $\boldsymbol{b}$-axis on the image plane. Analysing characteristic image features by using parameters in vector form, which are invariant to the coordinate inversion, is advantageous for determining the dislocation sign.

The essential point of our consideration is the replacement of the 'dislocation sign' in the sense of the $\boldsymbol{b}$ direction by another definition which is based on the orientation of the 'additional half plane' related to the optical axis and called 'dislocation parity' [13]. Based on a general consideration of contrast behaviour the modified method relates the inversion-independent parameters to the corresponding image features as, e.g., image shift or contrast oscillations.

2. Dislocation Parity

The Burgers vector $\boldsymbol{b}$ of a dislocation is known to be a pseudo-vector which is fixed only with respect to the dislocation line vector $\boldsymbol{l}$ (FS/RH rule) [11, 12]. Indeed, it changes the sign (direction) if $\boldsymbol{l}$ is inverted: $\boldsymbol{b} \rightarrow -\boldsymbol{b}$, if $\boldsymbol{l} \rightarrow -\boldsymbol{l}$. Thus, two pairs of vectors $(\boldsymbol{b}, \boldsymbol{l})$ and $(-\boldsymbol{b}, -\boldsymbol{l})$ characterize the same dislocation while $(\boldsymbol{b}, -\boldsymbol{l})$ and $(-\boldsymbol{b}, \boldsymbol{l})$ describe a different one, which is antiparallel. In this sense, the second dislocation is of opposite sign compared with the first one. For a pure screw dislocation $(\boldsymbol{b} \parallel \boldsymbol{l})$ the two different descriptions correspond to right-hand $(\boldsymbol{b} \cdot \boldsymbol{l} > 0)$ or left-hand $(\boldsymbol{b} \cdot \boldsymbol{l} < 0)$ screws, whereas for a pure edge dislocation $(\boldsymbol{b} \perp \boldsymbol{l})$ two opposite positions of the extra half plane in the crystal are presented [14] (see Fig. 1a).

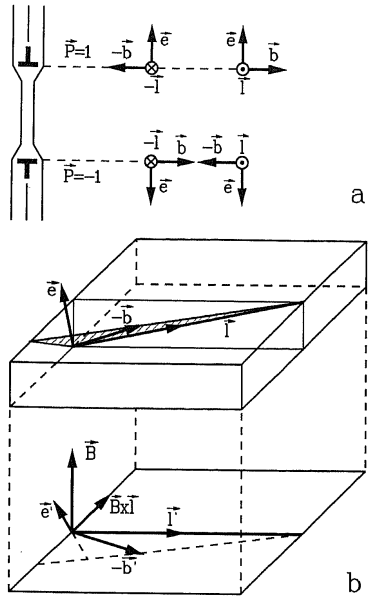

Fig. 1. Schemes of a) two different geometrical situations in a crystal with respect to the edge dislocations of opposite sign and b) the coordinate system in relation to the image of a crystal foil containing a mixed dislocation

The geometry of the dislocation within the crystal is invariant to the change of the coordinate system (e.g., $\boldsymbol{l}$ vector direction), hence, with $\boldsymbol{l}$ being fixed, $\boldsymbol{b}$ is unambiguously determined by the contrast analysis. For example, Marukawa [10] ascertained the respective $\boldsymbol{b}$ orientation by using the contrast asymmetry according to $\operatorname{sgn}(\boldsymbol{g} \cdot \boldsymbol{b})$ for fixed $\boldsymbol{l}$.

Föll and Wilkens [6] assumed the positive direction of the normal $\boldsymbol{n}$ to the plane of the dislocation loop and, hence, the positive $\boldsymbol{l}$ direction at each point of the loop in order to enable the unambiguous $\boldsymbol{b}$ vector determination by inside–outside contrast. In other words, they fixed the coordinate system so that the positive $\boldsymbol{b}$ direction with respect to $\boldsymbol{n}$ gets a certain physical meaning: $\boldsymbol{n} \cdot \boldsymbol{b} > 0$ was used for the vacancy loop and $\boldsymbol{n} \cdot \boldsymbol{b} < 0$ for the interstitial one.

For a single dislocation with a non-vanishing edge component, the normal $\boldsymbol{e} = \boldsymbol{l} \times \boldsymbol{b} / |\boldsymbol{l} \times \boldsymbol{b}|$ to the glide plane is a natural invariant parameter which is independent of the $\boldsymbol{l}$ direction chosen (see Fig. 1b). Vector $\boldsymbol{e}$ turns to the half space in the crystal with extra material, the additional lattice plane is characterized by the Burgers circuit. In the following this lattice half plane perpendicular to the edge component of $\boldsymbol{b}$ should be called the 'additional or extra half plane'. Contrary to $\boldsymbol{b}$ vector $\boldsymbol{e}$ is independent of the coordinate system chosen and, hence, is a real vector. Indeed, $\boldsymbol{e}(\boldsymbol{l}, \boldsymbol{b}) = \boldsymbol{e}(-\boldsymbol{l}, -\boldsymbol{b})$, but $\boldsymbol{e}(-\boldsymbol{l}, \boldsymbol{b}) = \boldsymbol{e}(\boldsymbol{l}, -\boldsymbol{b}) = -\boldsymbol{e}(\boldsymbol{l}, \boldsymbol{b})$.

It is advantageous to use vector $\boldsymbol{e}$ instead of $\boldsymbol{b}$ for characterizing the dislocation signs of edge and mixed dislocations. Sometimes the simple convention is used that an edge dislocation is considered positive if the $\boldsymbol{e}$ vector turns up, and negative if $\boldsymbol{e}$ turns down [14]. Especially for heterostructures the sign of the misfit dislocation is strongly connected with the misfit in the lattice parameters of the epilayer a_L and the substrate a_S. Indeed, the position of the additional half plane related to the interface normal $\boldsymbol{n}$ depends on the misfit sign yielding $(\boldsymbol{l} \times \boldsymbol{b} \cdot \boldsymbol{n}) < 0$ for $\Delta a = a_L - a_S > 0$, and vice versa.

In electron microscopy the vertical direction is related to the optical axis and can be fixed by the beam vector $\boldsymbol{B}$ which turns up to the electron gun, thus being perpendicular to the image plane. Therefore, the dislocation sign is controlled by the product of $\boldsymbol{B} \cdot \boldsymbol{e}$. Let the parameter $P = \operatorname{sgn}(\boldsymbol{B} \cdot \boldsymbol{e})$ be called dislocation parity because its value is defined as ± 1. The convention will be used that $P = +1$ characterizes the positive dislocation. A relation of the parity P to $\boldsymbol{b}$ may clearly be concluded from the equation $P = \operatorname{sgn}(\boldsymbol{B} \cdot \boldsymbol{e})$

$= \mathrm{sgn}\,(\boldsymbol{B}\cdot\boldsymbol{l}\times\boldsymbol{b}) = \mathrm{sgn}\,(\boldsymbol{B}\times\boldsymbol{l}\cdot\boldsymbol{b})$. For the positive dislocation, the projection of the $\boldsymbol{b}$ vector on the image plane turns to the same side of the dislocation line as that of vector $\boldsymbol{B}\times\boldsymbol{l}(\boldsymbol{B}\times\boldsymbol{l}\cdot\boldsymbol{b} > 0)$, i.e. it turns to the left side if looking along vector $\boldsymbol{l}$. Thus, to know the parity means to know the sign of the edge component of the $\boldsymbol{b}$ vector in the image plane for $\boldsymbol{l}$ fixed.

The limitations of the P definition are the following: first, the parity convention cannot be applied to pure screw dislocations ($|\boldsymbol{e}| = 0$), and second, it is uncertain if $\boldsymbol{e}\cdot\boldsymbol{B} = 0$. In the latter case vector $\boldsymbol{e}$ lies in the image plane ($\boldsymbol{b}$ is parallel to the $\boldsymbol{B}$-axis), however, it is also possible to define the dislocation sign by using another convention so that $\boldsymbol{g}\cdot\boldsymbol{e} > 0$ will correspond to a positive dislocation and $\boldsymbol{g}\cdot\boldsymbol{e} < 0$ to a negativ one.

The knowledge of the signs of $\boldsymbol{b}$ components both parallel and perpendicular to the image plane (P and $\mathrm{sgn}\,(\boldsymbol{g}\cdot\boldsymbol{e})$, respectively) is often sufficient to characterize $\boldsymbol{b}$ in most of the practical cases if a favourable type of $\boldsymbol{b}$ is known from crystallography and if the projection of $\boldsymbol{b}$ was determined by the invisibility condition for at least one $\boldsymbol{g}$ vector.

Our considerations are in accordance with a general description of the contrast behaviour (see, for example, [3]) of dislocations in isotropic media based on three contrast parameters $n = \boldsymbol{g}\boldsymbol{b}$, $p = \boldsymbol{g}\boldsymbol{b}_e$, $m = (\boldsymbol{g}\cdot\boldsymbol{b}\times\boldsymbol{l})/8$ (width, symmetry, visibility). The parity is similar to parameter n and the product of $\boldsymbol{g}\cdot\boldsymbol{e}$ is proportional to m. However, contrary to n the parity P is independent of the direction of $\boldsymbol{l}$ while $n = \boldsymbol{g}\cdot\boldsymbol{b}$ changes its sign for $\boldsymbol{l}\rightarrow -\boldsymbol{l}$. Such features as, e.g., halo contrast, image shift and black–white oscillations are known to be controlled by the dislocation sign [2]. Therefore, the parity can be determined by the use of contrast effects, which are sensitive to n, for instance, image shift with respect to the dislocation line [4 to 6, 15] or oscillating contrast [10], while sign $(\boldsymbol{g}\cdot\boldsymbol{e})$ can be revealed by means of residual (halo) contrast, which is sensitive to m [7, 8] (see Table 3).

Experimental and theoretical studies of dislocation contrast were carried out in order to demonstrate the application of the parity analysis to the Burgers vector determination.

3. Experimental and Simulation Technique

A number of threading dislocations in a GaAlAs/GaAs (001) double heterostructure have been used for contrast experiments, carried out at the JEOL JEM 1000 electron microscope at an accelerating voltage of 1 MV. The heterostructure has been grown by liquid phase epitaxy (LPE) under standard conditions pointed out in [16, 17]. The electron microscope specimens were first prepared by chemical polishing followed by ion milling down to a thickness of about 0.45 μm. Image simulations were performed using the two-beam approximation of dynamical scattering in the Howie-Whelan formulation (see, e.g., [3]).

4. Results and Discussion

Fig. 2 to 5 represent electron microscope micrographs and corresponding simulated images of two dislocations (A and B) under different diffraction conditions. The $\boldsymbol{B}$ vector was approximately parallel to [001] and differed from this direction by not more than 3° to 5° in the contrast experiments. The normal $\boldsymbol{F}$ to the upper thin foil surface was approximately parallel to [001], too, and the foil looked like a plate. A stereo pair was prepared to study the spatial arrangement of dislocations in the foil. In accordance with Head et al. [9] positive $\boldsymbol{l}$ directions of these inclined dislocations were chosen to be turned up.

Conventional diffraction analysis has been applied to determine all parameters of these dislocations. First, in accordance with the zincblende structure of AlGaAs the most

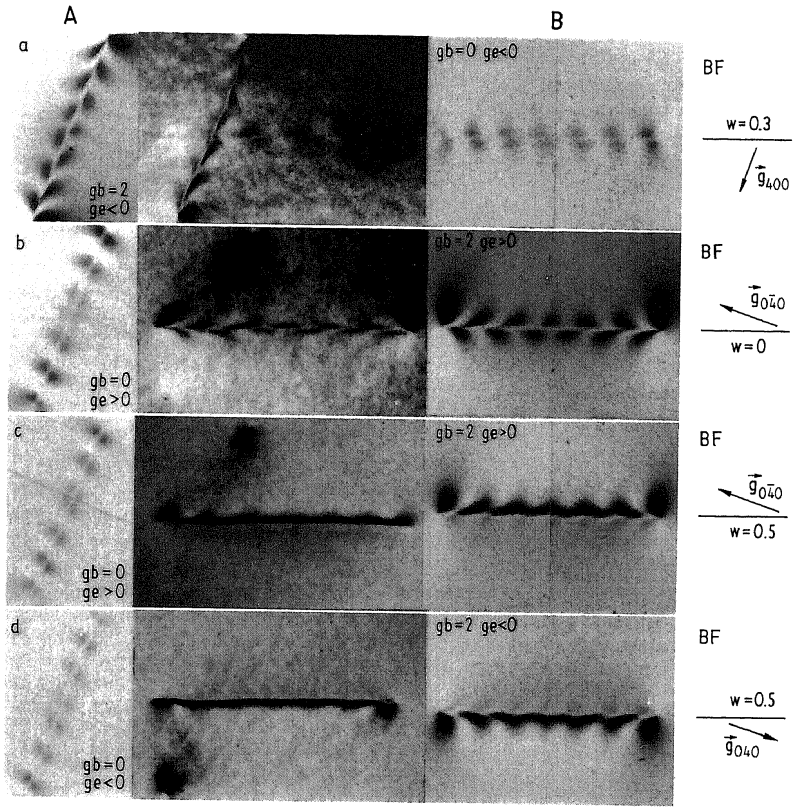

Fig. 2. a) to d) Experimental (central column) and calculated electron microscope images of dislocations A and B under $\boldsymbol{g}$ excitation of ⟨400⟩ type for different w values

favourable type of the Burgers vector is $(a/2)\langle 110\rangle$. Then, using the invisibility criterion revealed that the projection of the b-axis is parallel to [100] (dislocation A, Fig. 2, b to d) or [010] (dislocation B, Fig. 2a). Optimum fitting of the calculated images to the experimental ones yielded the unique Burgers vectors of $(a/2)$ [101] and $(a/2)$ $[0\bar{1}\bar{1}]$ for A and B dislocations, respectively, with some other parameters, e.g., foil thickness t, dislocation line vector $\boldsymbol{l}$, deviation parameter w, etc., being refined. The resulting geometrical parameters of the dislocations and diffraction conditions corresponding to Fig. 2 to 5 are shown in Tables 1 and 2, respectively. The dislocations under investigation have a mixed character with a large screw component (the angles between $\boldsymbol{b}$ and $\boldsymbol{l}$ vectors are in the range of 8° to 15°) and the same slip plane $(\bar{1}\bar{1}1)$, i.e. the same $\boldsymbol{e}$ vector. Thus, the image series in Fig. 2 to 5 enable us to get an impression of the contrast behaviour of the mixed dislocations in dependence on diffraction conditions and dislocation parities.

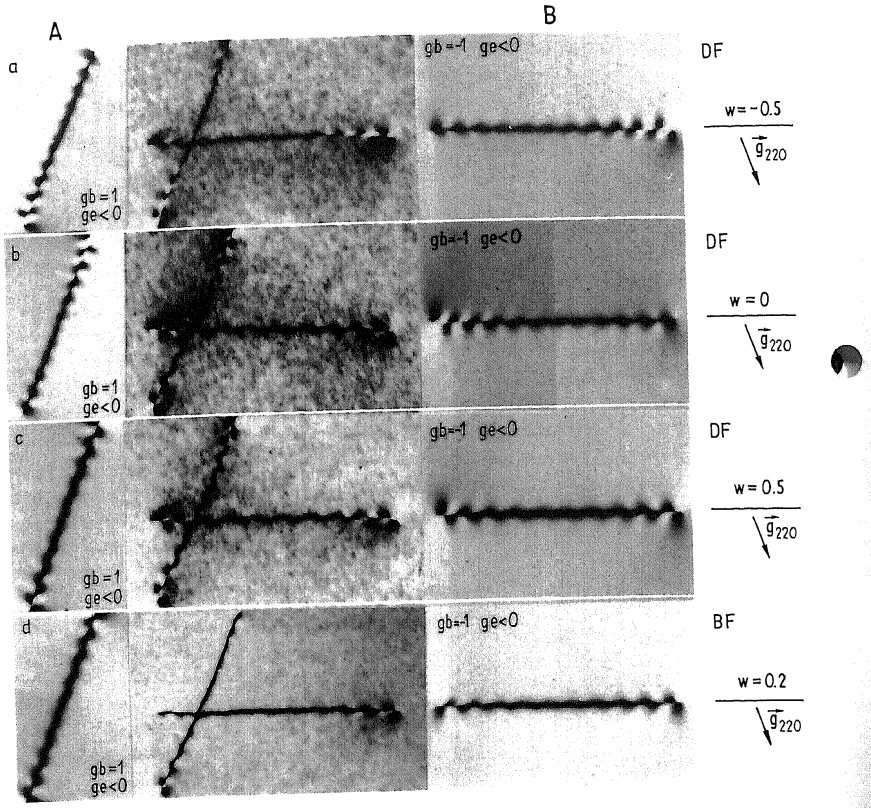

Fig. 3. a) to d) Experimental (central column) and calculated electron microscope images of dislocations A and B under $\boldsymbol{g} = [220]$ for different w values

In order to apply the vector formalism to contrast analysis (see Table 3) it is first necessary to choose the coordinate system and, second, to define the contrast vectors. The natural coordinate system related to the dislocation image can be created by $\boldsymbol{l}' = \boldsymbol{x}$, $\boldsymbol{B} = \boldsymbol{z}$, and the respective vector product $\boldsymbol{B} \times \boldsymbol{l} = \boldsymbol{y}$, where $\boldsymbol{l}'$ is the projection of $\boldsymbol{l}$ on the image plane (Fig. 1b).

4.1 Oscillating contrast

The majority of the dislocation images in Fig. 2 to 5 demonstrate the strongly oscillating contrast owing to the inclination of dislocation lines to the foil surface. Oscillations are stronger at $w = 0$ (see, for example, Fig. 2b and 3b, c) and become weaker with increasing $|w|$, in particular, for $|n| = 2$ (Fig. 2c, d). The deviation parameter is $w = s\xi_g$, where s is the excitation error and ξ_g is the extinction distance [1].

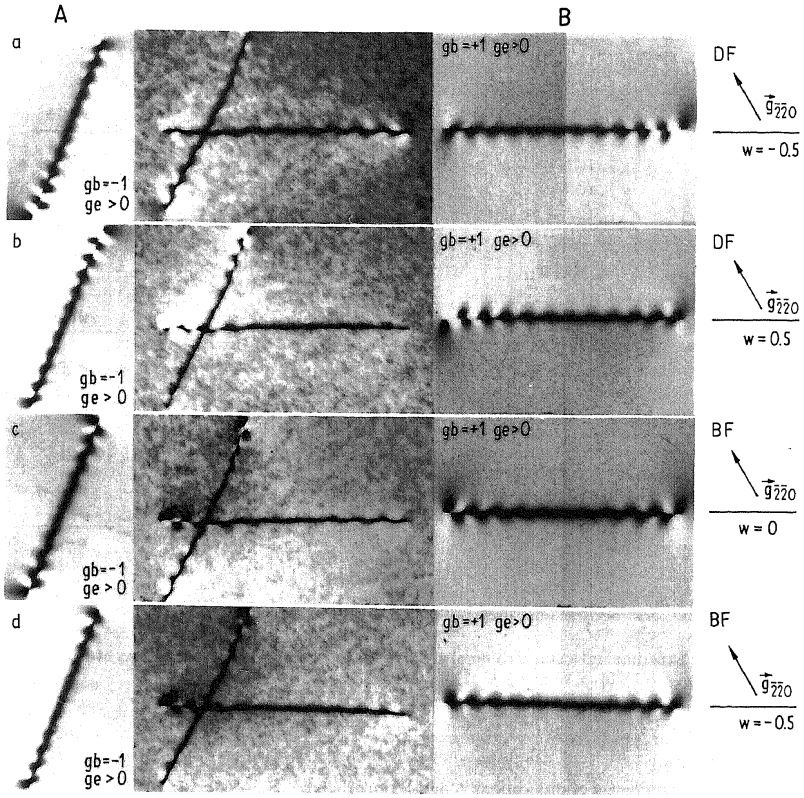

Fig. 4. a) to d) Experimental (central column) and calculated electron microscope images of dislocations A and B under $\boldsymbol{g} = [\bar{2}\bar{2}0]$ for different w values

Based on the similarity of the oscillating contrast of inclined dislocations to the contrast of the straight arrangement of precipitates it is possible to define the contrast vector $\boldsymbol{\Delta}_0$, which goes from the centre of a black dot to that of a white dot at the point of emergence of the dislocation at the surfaces (see Fig. 6). This is similar to the black-and-white vector used in analysing the precipitates [18]. As the images show, vector $\boldsymbol{\Delta}_0$ is independent of w, but changes its direction for $\boldsymbol{g} \to -\boldsymbol{g}$. In accordance with the symmetry properties of dislocation images vectors $\boldsymbol{\Delta}_0$ at the top and bottom points of emergence are parallel in bright field images and antiparallel in dark field ones. The dependence of vector $\boldsymbol{\Delta}_0$ on dislocation and contrast parameters (see Table 2) is described by

$$\boldsymbol{\Delta}_0 = n[\boldsymbol{l} \times \boldsymbol{B}] . \tag{1}$$

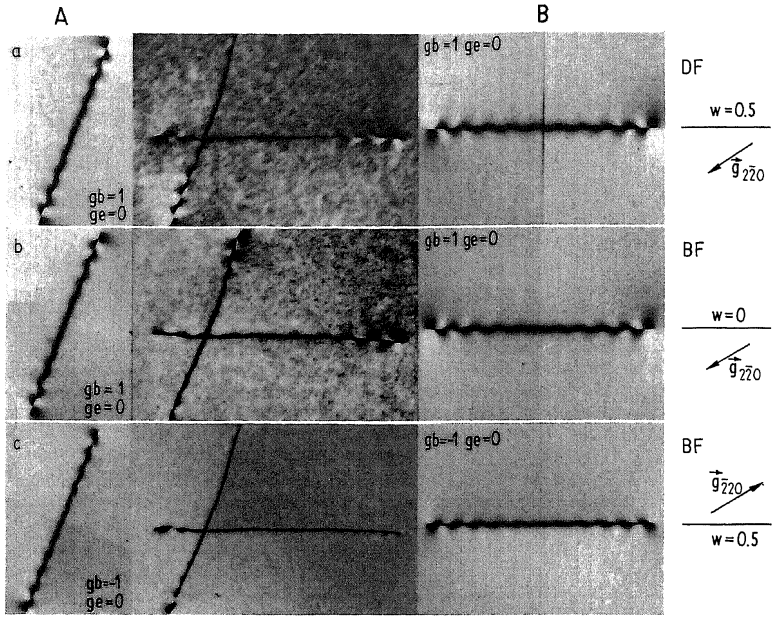

Fig. 5. a) to c) Experimental (central column) and calculated electron microscope images of dislocations A and B under $\boldsymbol{g} = [2\bar{2}0]$ (a, b) and $\boldsymbol{g} = [\bar{2}20]$ (c) for different w values

Table 1
The parameters of dislocations A and B under study

dislocation	$\boldsymbol{l}$ [hkl]	$\boldsymbol{b}$ [hkl]	$\boldsymbol{e}$ [hkl]
A	$[7\bar{1}6]$	$(a/2)\,[101]$	$[\bar{1}\bar{1}1]$
B	$\approx[\bar{1}32]$	$(a/2)\,[0\bar{1}\bar{1}]$	$[\bar{1}\bar{1}1]$

Table 2
Diffraction conditions related to Fig. 2 to 5

dis-loc.	$\boldsymbol{g}_{400}$ n	(Fig. 2a) sgn (m)	$\boldsymbol{g}_{0\bar{4}0}$ n	(Fig. 2b) sgn (m)	$\boldsymbol{g}_{220}$ n	(Fig. 3) sgn (m)	$\boldsymbol{g}_{\bar{2}\bar{2}0}$ n	(Fig. 4) sgn (m)	$\boldsymbol{g}_{2\bar{2}0}$ n	(Fig. 5a, b) sgn (m)	P
A	2	−1	0	+1	+1	−1	−1	+1	+1	0	1
B	0	−1	2	+1	−1	−1	+1	+1	+1	0	1

Table 3
Contrast features of dislocation images in dependence on the dislocation parameters and diffraction conditions

contrast	contrast parameter	dependence	validity region	parity P	limitations
contrast oscillations near the surface	Δ_0: black–white vector, drawn from the centre of the black spot to the centre of the dark one at the end of dislocation oscillation contrast	$\Delta_0 = -(\boldsymbol{g}\cdot\boldsymbol{b})\,[\boldsymbol{B}\times\boldsymbol{l}]$	inclined dislocation, $\boldsymbol{g}\cdot\boldsymbol{b} \neq 0$, BF: both ends, DF: top end, bottom reversed	$-\operatorname{sgn}(g_1\Delta_0)$	g_1 belongs to one of two largest ($>90°$) solid angles bounded by $\boldsymbol{l}'$ and $\boldsymbol{g}_0$ axes
image shift	Δ: shift vector drawn normal to the dislocation line towards the minimum of the average image intensity	$\Delta = (n/\xi_g)\operatorname{sgn}(s)\sqrt{1+1/w^2}\,[\boldsymbol{B}\times\boldsymbol{l}]$	$\boldsymbol{g}\cdot\boldsymbol{b} \neq 0$, $w \neq 0$	$\operatorname{sgn}(g_1\Delta w)$	the same as above
halo contrast	I_H: brightness of the extended halo around the point of emergence of a dislocation at a surface	$I_H > I_0$ if $\boldsymbol{g}\cdot\boldsymbol{e} > 0$ (white halo) $I_H < I_0$ if $\boldsymbol{g}\cdot\boldsymbol{e} < 0$ (black halo)	$\lvert w\rvert \leqq 0.3$, DF: both surfaces, BF: top surface, bottom reversed		

Equation (1) is limited to cases with $n = \boldsymbol{g} \cdot \boldsymbol{b} \neq 0$ or $[\boldsymbol{B} \times \boldsymbol{l}] \neq \boldsymbol{0}$. Equation (1) is in good agreement with Marukawa's conclusion [10]: when looking along vector $\boldsymbol{l}$ the first dark contrast appears on the left of the dislocation line if $\boldsymbol{g} \cdot \boldsymbol{b} > 0$, and on the right if $\boldsymbol{g} \cdot \boldsymbol{b} < 0$. Indeed, it is known (see, e.g., [2]) that in the bright field images the contrast at the point of emergence of a dislocation at a surface is white if $\boldsymbol{g}(\mathrm{d}\boldsymbol{R}/\mathrm{d}z) > 0$, and dark if $\boldsymbol{g}(\mathrm{d}\boldsymbol{R}/\mathrm{d}z) < 0$.

4.2 Image shift in respect of the dislocation line

The changes of contrast on both sides of a dislocation line are asymmetric: the contrast on one side is stronger than on the other for $w \neq 0$ [1, 2]. This means that the middle line of the contrast is shifted with respect to the dislocation line. The shift can be characterized by a vector $\boldsymbol{\Delta}$, which is perpendicular to the projection of the dislocation line $\boldsymbol{l}$ on the image plane (Fig. 6). The dependence of $\boldsymbol{\Delta}$ on dislocation and diffraction parameters can be roughly described [15] by

$$\boldsymbol{\Delta} \sim (\boldsymbol{g} \cdot \boldsymbol{b})\, w[\boldsymbol{B} \times \boldsymbol{l}]\,. \tag{2}$$

Owing to the existence of a small spacing between the intensity peak position and the projection of the dislocation line also at $w = 0$ the dependence of $\boldsymbol{\Delta}$ should be modified

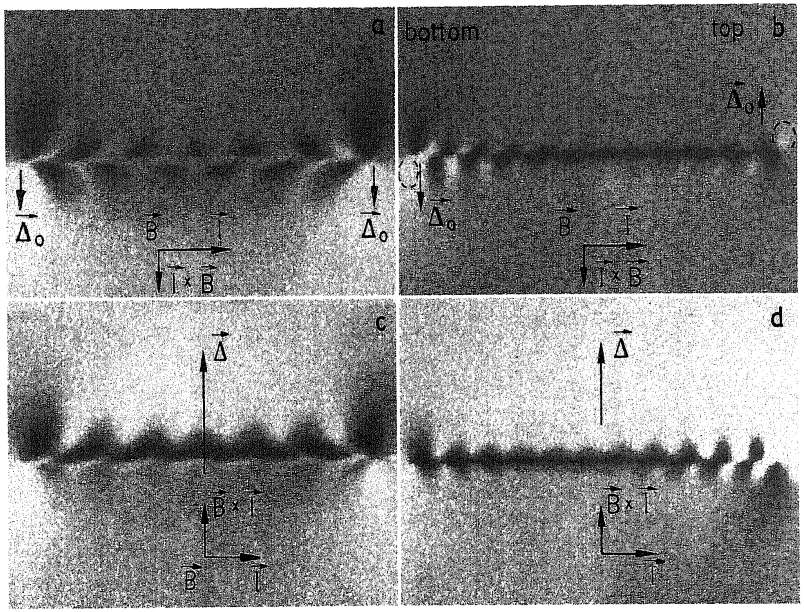

Fig. 6. Characterization of the image features by the contrast vectors. Oscillation contrast: a) BF image, $\boldsymbol{g} \cdot \boldsymbol{b} = 2$, $w = 0$ and b) DF image, $\boldsymbol{g} \cdot \boldsymbol{b} = -1$, $w = 0$; image shift: c) BF image, $\boldsymbol{g} \cdot \boldsymbol{b} = 2$, $w > 0$ and d) DF image, $\boldsymbol{g} \cdot \boldsymbol{b} = -1$, $w < 0$

yielding

$$\boldsymbol{\Delta} = (n/\xi_{\boldsymbol{g}})\, \mathrm{sgn}\,(s) \sqrt{1 + w^2}\, [\boldsymbol{B} \times \boldsymbol{l}]\,. \tag{3}$$

For $|n| = |\boldsymbol{g} \cdot \boldsymbol{b}| = 2$ and $w \neq 0$ (see, for example, Fig. 2c, d) the direction of the image shift can directly be evaluated from the micrographs. It is obvious that if $\boldsymbol{l} \to -\boldsymbol{l}$, $[\boldsymbol{B} \times \boldsymbol{l}]$ and $\boldsymbol{g} \cdot \boldsymbol{b}$ change their signs simultaneously so that vector $\boldsymbol{\Delta}$ will still be the same. If the $\boldsymbol{B}$ vector changes its direction (for instance, by turning the sample in the holder) under the same diffraction conditions vector $\boldsymbol{\Delta}$ will also reverse its direction. Using (2) or (3) enables one to determine sgn (n) by comparing the $\boldsymbol{\Delta}$ direction with the $[\boldsymbol{B} \times \boldsymbol{l}]$ vector (Fig. 6).

4.3 Halo contrast

This type of contrast was investigated in detail both experimentally and theoretically for pure edge dislocations [7, 8]. Almost all images with $\boldsymbol{g} \cdot \boldsymbol{e} \neq 0$ show (see, for example, Fig. 3, 4) a distinct halo contrast, in particular, near the point of emergence of the dislocation at the surface, in spite of the dislocations having a relatively small contribution of the edge component of $\boldsymbol{b}$. The influence of screw component on the halo contrast is not sufficiently clarified and will be investigated in detail in future. Furthermore, in the case of pure screw dislocations the b-axis can already completely be determined by an invisibility criterion. Nevertheless the main properties of the halo contrast, which are deduced from the micrographs, seem to be very similar to those for pure edge dislocations [7, 8]. They are as follows:

1. In the images of dislocation segments situated near the foil surface the halo contrast is observed to be the stronger, the closer the dislocation is to the surface. The intensities of the halos are highest for $w > 0$ if the dislocation lies near the bottom surface, and for $w < 0$ if the dislocation lies near the top one.

2. The halo contrast is observed in both dark and bright fields. The type of the halo (dark or bright) strongly depends on the sign of $(\boldsymbol{g} \cdot \boldsymbol{b} \times \boldsymbol{l})$ and is independent of the dislocation position in the foil in the dark field. In the bright field, the halo has the same brightness as in the dark field if the dislocation is situated near the top surface; it is of opposite brightness if the dislocation is situated near the bottom surface.

Therefore the behaviour of the halo contrast enables us to determine the projection of $\boldsymbol{e}$ on the image plane in a simple way:

$$\begin{aligned} &\boldsymbol{g} \cdot \boldsymbol{e} > 0 \quad \text{if the halo contrast is bright,} \\ &\boldsymbol{g} \cdot \boldsymbol{e} < 0 \quad \text{if the contrast is dark} \end{aligned} \tag{4}$$

for both points of emergence of a dislocation in dark field and of an upper dislocation surface in bright field (see Table 2). For the bottom point of emergence of a dislocation in the bright field the halo contrast is reversed.

4.4 Methods of Burgers vector determination

In order to determine the Burgers vector $\boldsymbol{b}$ of an arbitrary single dislocation, several vectors probable for $\boldsymbol{b}$ should be deduced first by means of object crystallography. In general, three different ways can be used to reduce the residual freedom in the $\boldsymbol{b}$ space so that only one $\boldsymbol{b}$ vector will be chosen.

The first way is very similar to Marukawa's method [10]: analysing the contrast features (oscillations, image shift, halos) under different $\boldsymbol{g}$ vectors in accordance with the vector formulas in Table 2 reduces a solid angle for the probable $\boldsymbol{b}$ orientation thus enabling a

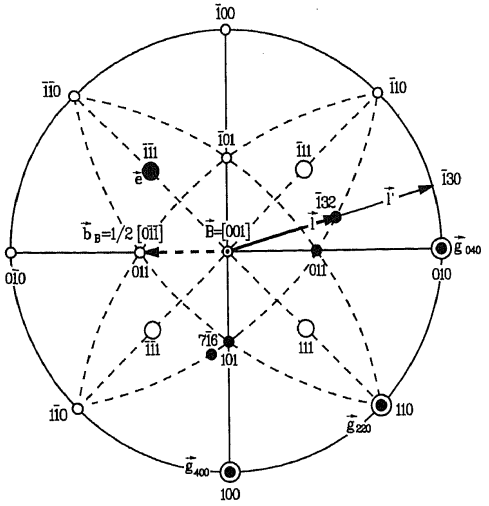

Fig. 7. Stereographic (001) projection of a cubic crystal. The normal to foil F and beam vector B are close to the interface normal [001]. g_{400}, g_{040}, g_{220} are the diffraction vectors which are used in the micrographs of Fig. 2a, 2d, 3, respectively. The line l of dislocation B, its projection l' on the image plane and Burgers vector b are also indicated

unique b to be gained. At least, two experimental micrographs taken at different g reflections are necessary to identify b. In the first image, at g_1 one can arbitrarily choose the direction of dislocation line l' and then draw the vector of $[B \times l]$ (see Fig. 6). By examining the contrast features in accordance with the formulas in Table 3, the sign of $g_1 \cdot b$ can be determined as follows:

$$\operatorname{sgn}(g_1 \cdot b) = \operatorname{sgn}(\Delta \cdot B \times l) \operatorname{sgn}(w) \tag{5a}$$

or

$$\operatorname{sign}(g_1 \cdot b) = -\operatorname{sgn}(\Delta_0 \cdot B \times l). \tag{5b}$$

Now the possible orientation of b is limited by half the space, i.e., the Burgers vector b belongs to a hemisphere with g_1 being the pole of the stereographic sphere (see Fig. 7 and 8). The same procedure can be applied to the second image at g_2, and, hence, the space of the b orientation possible will be further limited: b belongs to the common area of the two hemispheres with g_1 and g_2 being the poles. Using a number of images, one can deduce the space of the b orientations possible so that the Burgers vector can be chosen unambiguously from crystallographically allowable vectors.

This procedure is illustrated by the scheme in Fig. 8 (row I) using an example of two images of dislocation B shown in Fig. 2d and 3a. Owing to the favourable glide system for AlGaAs which is ⟨110⟩ (111), the number of possible b vectors of (1/2) ⟨110⟩ type is twelve taking into account the vector sign (Ia, Fig. 8). Both the oscillations and image shift in the micrograph for $g = [040]$ in Fig. 2d indicate $g_1 \cdot b < 0$ ($g_1 \cdot b = -2$) for the given direction of $l' = [\bar{1}30]$ (from left to right in the image of Fig. 2d) since $\operatorname{sgn}(\Delta \cdot B \times l) \operatorname{sgn}(w) = -1$ as well as $-\operatorname{sgn}(\Delta_0 \cdot B \times l) = -1$ (see (5a), (5b) respectively). The orientations of the vectors mentioned above are also shown in stereographic projection in Fig. 7. Four of the twelve vectors, viz. (1/2) $[\bar{1}\bar{1}0]$, (1/2) $[1\bar{1}0]$, (1/2) $[0\bar{1}1]$, (1/2) $[0\bar{1}\bar{1}]$, satisfy the requirement of $g \cdot b < 0$ (see Ib, Fig. 8). Vectors (1/2) [101], (1/2) $[\bar{1}0\bar{1}]$, (1/2) $[\bar{1}01]$, (1/2) $[10\bar{1}]$, for which $g \cdot b = 0$,

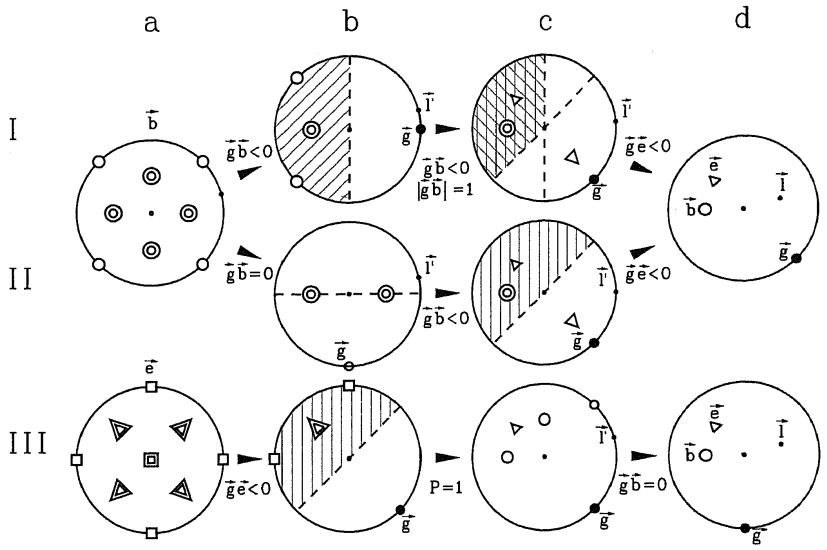

Fig. 8. Schemes of three possibilities (rows I to III) of determining b by using of the contrast feature analysis. In the first two ways (I and II), the Burgers vector is chosen from twelve vectors of ⟨110⟩ type possible for b, which are in the stereographic projection shown as open circles (○). The size of the symbols depends on the vector position with respect to the image plane increasing for vectors running downwards. In the last method (III), both the eight vectors of ⟨111⟩ type (△) and the six vectors of ⟨100⟩ type (□) possible of e are considered in order to determine e unambiguously by applying sgn $(g \cdot e)$ and the parity analysis. Diffraction vectors g, dislocation line l and its projection on the image plane l' are also shown as dark spots

are excluded from the contrast features. By examining the image shift in a further image with $g = [220]$ the possible b orientation is reduced to two vectors, viz. (1/2) $[0\bar{1}1]$ and (1/2) $[0\bar{1}\bar{1}]$ (see Ic, Fig. 8) since two other vectors, viz. (1/2) $[\bar{1}\bar{1}0]$ and (1/2) $[1\bar{1}0]$, correspond to $g \cdot b = -2$ and $g \cdot b = 0$, respectively.

From the eight vectors of ⟨111⟩ type possible for e, which are the normals to the (111) slip planes, two vectors, $[\bar{1}\bar{1}1]$ and [111] (see Ic, Fig. 8), can be chosen, which correspond to both pairs of $b = (1/2)[0\bar{1}\bar{1}]$, $l = [\bar{1}32]$ and $b = (1/2)[01\bar{1}]$, $l = [\bar{1}3\bar{2}]$ ($[\bar{1}32]$ and $[\bar{1}3\bar{2}]$ have the same projection of $[\bar{1}30]$ on the (001) plane). The dark halo contrast (DF image) indicates $g \cdot e = (g \cdot l \times b) < 0$. Therefore, $e = [\bar{1}\bar{1}1]$ and, finally, $b = (1/2)[0\bar{1}\bar{1}]$ (Id, Fig. 8).

Contrary to Marukawa's method this procedure enables us to determine vector b without a large inclination of the sample in the microscope during the contrast experiment. Moreover, it can also be applied to the dislocation lying parallel to the foil surface.

The second way illustrated by row II in Fig. 8 is related to the reduction of the probable b orientation by applying the $g \cdot b = 0$ method. If the projection of the b-axis on the image plane is known from the invisibility criterion for one g_0 vector (see Ib, Fig. 8), b can further be determined by the analysis of the contrast features requiring fewer images. For example, Fig. 2a represents the weak image of dislocation B which corresponds to a vanishing contrast

owing to $g_0 \cdot b = 0$. The residual contrast is the result of $(g_0 \cdot b \times l) \neq 0$. Of this image four possible b vectors, viz. (1/2) [0$\bar{1}$1], (1/2) [01$\bar{1}$], (1/2) [011], (1/2) [0$\bar{1}\bar{1}$], satisfy the requirement of $g \cdot b = 0$ (Ib, Fig. 8). Using the contrast features of the image in Fig. 3a (IIc, Fig. 8) enables the unique b vector of (1/2) [0$\bar{1}\bar{1}$] to be concluded as shown above (IId, Fig. 8).

4.5 *Parity analysis*

In the third way, the e vector defined by parity and sgn $(g \cdot e)$ analysis is used instead of the direct b determination (see Table 3 and row III in Fig. 8).

In the particular case of $g_1 \perp g_0$, i.e. $g_1 \parallel b'$ where b' is the projection of the b vector on the image plane and g_0 is the diffraction vector satisfying the invisibility criterion, the parity can be directly related to the image shift and the black-and-white vector (see Table 3). The relation of P to the $[B \times l]$ vector, viz. sgn $(B \times l \cdot g_1)$ = sgn $(B \times l \cdot b)$ sgn $(g_1 \cdot b)$ = P sgn $(g_1 \cdot b)$, can easily be obtained by taking into account that sgn $(A \cdot g_1)$ = sgn $(A \cdot b)$ × sgn $(g_1 \cdot b)$ for g_1 and arbitrary A vectors. Thus, the black-and-white vector Δ_0 is related to P yielding

$$\begin{aligned} \operatorname{sgn}(-\Delta_0 \cdot g_1) &= \operatorname{sgn}(g_1 \cdot b) \operatorname{sgn}(B \times l \cdot g_1) = \operatorname{sgn}^2(g_1 \cdot b) \operatorname{sgn}(B \times l \cdot b) \\ &= \operatorname{sgn}(B \times l \cdot b) = P, \end{aligned} \tag{6}$$

and one can find a relation similar to the image shift Δ (see Table 3).

Equation (6) holds good also if g_1 belongs to one of the two largest solid angles made by l' and g_0. It shows that the parity is connected unambiguously with both the contrast properties (image shift, oscillations, etc.) and the position of the extra half plane with respect to the normal B to the image plane. That means e points towards $\pm B$ for $P = \pm 1$, conserving the FS/RH convention. Thus, the analysis of both the contrast features and the parity enables us to unify the Burgers vector determination being independent of the orientation of l and the coordinate system, respectively. Similar to this, using the halo contrast enables sgn $(g_1 \cdot e)$ and, thus, the orientation of e in the image plane to be determined.

The examples of Figures 2a and 3a are also used to illustrate the above (see row III, Fig. 8). Examining the halo contrast in the image of dislocation B in Fig. 3a reveals two vectors, viz. [$\bar{1}\bar{1}\bar{1}$] and [$\bar{1}\bar{1}$1] (IIIb, Fig. 8), possible for e, which satisfy the requirement of $g \cdot e < 0$ and which can be chosen from the eight vectors of ⟨111⟩ type, which are the crystallographically allowable vectors (IIIa, Fig. 8). Four vectors, viz. [1$\bar{1}$1], [$\bar{1}$1$\bar{1}$], [$\bar{1}$11], [1$\bar{1}\bar{1}$], which correspond to $g \cdot e = 0$, are excluded. Taking into account the dislocations with a glide plane of (001) type, which can be a result of dislocation reaction, two vectors, viz. [0$\bar{1}$0] and [$\bar{1}$00], can also be considered (see IIIb, Fig. 8) because those satisfy the requirement mentioned above. The image shift in Fig. 3a indicates $P = 1$ since sgn $(g_1 \cdot \Delta)$ = 1. Therefore, $e = [\bar{1}\bar{1}1]$ (IIIc, Fig. 8).

Of the six vectors of ⟨110⟩ type lying in the $(\bar{1}\bar{1}1)$ slip plane, three vectors, viz. [$\bar{1}$10], [$\bar{1}$0$\bar{1}$], [0$\bar{1}\bar{1}$], correspond to $e = [\bar{1}\bar{1}1]$ if $l' = [\bar{1}30]$ ($l = [\bar{1}32]$ see IIIc, Fig. 8). The vector of [0$\bar{1}\bar{1}$] only satisfies the requirement of $g_0 \cdot b = 0$ for $g_0 = [040]$ in Fig. 2a. Thus, $b = (a/2)$ × [0$\bar{1}\bar{1}$] if $l = [\bar{1}32]$ (see IIId, Fig. 8 and Table 1). Dislocation A can be analysed analogously.

The algorithm of the parity analysis can therefore be summarized as follows. According to the object crystallography several axes probable for an e vector can be concluded from this. Then, analysing the contrast features (see Table 3) in an image with $g_1 \cdot b \neq 0$ one can define the dislocation parity P and, hence, vector e. By applying the invisibility criterion

$g_0 \cdot b = 0$ for one g_0 vector the unique vector b can finally be chosen from several vectors lying in a slip plane with the normal e if the l direction is fixed. Two images only are often sufficient to determine the parity and the Burgers vector of the dislocation.

4.6 *Discussion*

The main advantages of the method proposed lie in the choice of the spatial position of the vector e to characterize the dislocation sign as well as in the use of the contrast analysis with vector form parameters. Indeed, the theoretical consideration, or the model for image simulation, always chooses the coordinate system in agreement with certain conventions (see Section 2). In the experimental practice this can be done arbitrarily thus implying some uncertainties in determining the b direction [4, 5]. In order to avoid them, e.g., in the inside–outside contrast method the positive l direction was defined by fixing the positive direction of the normal n to the dislocation loop [6]. In our method of considering straight dislocations the parity is directly connected with the orientation of vector e and it is independent of the choice of coordinate l. On the other hand, the vector form of the dependencies of contrast parameters on dislocation characteristics and diffraction conditions is rather suitable for contrast analysis in the general case.

The modified analysis of Burgers vectors can be applied, e.g., to dislocations in semiconductors where only parts of loops are visible so that the inside–outside technique fails. The investigation of a lot of dislocations such as, e.g., A and B reveals that dislocations having the same glide planes are created in deformation centres at the interface under residual stresses during growth or postgrowth cooling. The nature of such deformation centres was discussed elsewhere [17] and can be associated with the small Al_2O_3 precipitates in AlGaAs epilayers. Dislocation loops gliding from the centre to the surface grown break into two segments which are almost parallel to the Burgers vector b. Therefore, most of the threading dislocations observed in epilayers have a large screw component of b. Dislocations A and B represent two segments of different dislocation loops starting from the same deformation centre.

The results described above showing the generalization of the dislocation sign enable us to simplify the conventional diffraction contrast analysis for arbitrary single dislocations.

Acknowledgements

The authors are gratefully indebted to Prof. J. Heydenreich, Dr. D. Baither, and Dr. U. Richter for helpful discussions as well as to the Max Planck Society (S. S. Ruvimov) and to the Stiftung Volkswagenwerk for financial support.

References

[1] A. HOWIE and M. J. WHELAN, Proc. Roy. Soc. A **263**, 217 (1961); **267**, 206 (1962).
[2] P. B. HIRSCH, A. HOWIE, R. B. NICOLSON, D. W. PASHLEY, and M. J. WHELAN, Electron Microscopy of Thin Crystals, Butterworth, London, 1965.
[3] K. SCHEERSCHMIDT, in: Electron Microscopy in Solid State Physics, Ed. H. BETHGE and J. HEYDENREICH, Elsevier Publ. Co., Amsterdam 1987 (p. 535).
[4] G. W. GROVES and A. KELLY, Phil. Mag. **6**, 1527 (1961); **7**, 892 (1961).
[5] P. M. KELLY and R. G. BLAKE, Phil. Mag. **28**, 475 (1973).
[6] H. FÖLL and M. WILKENS, phys. stat. sol. (a) **31**, 519 (1975).
[7] V. N. ROSHANSKII, I. A. RAGIMOV, K. SCHEERSCHMIDT, and J. HEYDENREICH, Fiz. tverd. Tela **17**, 2705 (1975); **23**, 256 (1981).